Double Dative Bond Configuration: Pyrimidine on Ge(100)

Jun Young Lee,[†] Soon Jung Jung,[†] Suklyun Hong,*[,‡] and Sehun Kim*[,†]

Department of Chemistry and School of Molecular Science (BK 21), Korea Advanced Institute of Science and Technology, Daejeon 305-701, Republic of Korea, and Department of Physics, Sejong University, Seoul, 143-747, Republic of Korea

Received: July 9, 2004; In Final Form: October 1, 2004

The adsorption of pyrimidine onto Ge(100) surfaces has been investigated using real-time scanning tunneling microscopy (STM), temperature-programmed desorption (TPD), and density-functional theory (DFT) calculations. Our results show that the adsorbed pyrimidine molecules are tilted about 40° with respect to the Ge surface, and through a Lewis acid−base reaction form bridges between the down-Ge atoms of neighboring Ge dimer rows by double Ge−N dative bonding without loss of aromaticity. For coverages of pyrimidine up to 0.25 ML, a well-ordered c(4×2) structure results from states that appear in STM micrographs as oval-shaped protrusions, which correspond to pyrimidine molecules datively adsorbed on every other dimer. However, above 0.25 ML, the oval-shaped protrusions gradually change into brighter zigzag lines. At 0.50 ML, a p(2×2) structure results from the states that appear in STM as zigzag lines. The zigzag lines are formed by the attachment of pyrimidine molecules to the down-Ge atoms of every Ge dimer. However, the unstable p(2×2) structure eventually reconstructs into a c(4×2) structure due to steric hindrance between the adsorbed pyrimidine molecules after stopping the exposure of pyrimidine to the surface.

Introduction

The adsorption of organic molecules onto Si(100) and Ge(100) surfaces is of both fundamental and technological importance because the formation of well-ordered organic layers on these surfaces is expected to have a wide range of applications in molecular electronics and biosensing devices.[1−4] Recent studies have significantly enhanced our understanding of the interaction of functional organic molecules with semiconductor (100) surfaces.[5−13] Si(100) and Ge(100) surfaces undergo a 2×1 reconstruction in which adjacent Si and Ge atoms pair up to form a dimer held together by a strong σ bond and a weak π bond, similar to C═C bonds in alkenes. The dimer is buckled by charge transfer from one atom, the buckled-down atom, to the other atom, the buckled-up atom. Hence, the electron density at the up atom is higher than that at the down atom, making the up atom an electron donor and the down atom an electron acceptor. The electronic properties of Si(100) and Ge(100) surfaces facilitate a number of adsorption reactions that attach organic molecules to them, such as cycloaddition or Lewis acid−base reactions,[1,5−13] as illustrated in Figure 1a and b.

Until now, studies in this area have primarily concentrated on the covalent attachment of functional organic molecules to Si(100) and Ge(100) surfaces through cycloaddition reactions.[6−10] A number of experimental and theoretical studies have shown that unsaturated organic molecules, including alkenes and cyclic dienes such as ethylene, cyclopentadiene, cyclohexadiene, and several benzene derivatives, attach to Si and Ge dimers via [2+2] cycloadditions or [4+2] Diels−Alder reactions.[5−13] The attachment of organic molecules to these surfaces through Lewis acid−base reactions has also recently been investigated. Previous studies have shown that N-containing organic molecules, including pyridine and several alkylamines, interact with Si(100) and Ge(100) surfaces by dative bonding between the N atom and the down atom of a dimer, where the N-atom with its lone pair of electrons acts as the Lewis base and the down atom of the dimer acts as the Lewis acid.[14−17] Recent scanning tunneling microscopy (STM) results have shown that pyridine molecules attach to the electron-deficient down-Ge atoms of Ge(100) via Ge−N dative bonding to form perfectly ordered organic monolayers without loss of aromaticity.[18] These STM results show that Lewis acid−base reactions can be used in novel schemes for the formation of well-ordered organic monolayers.

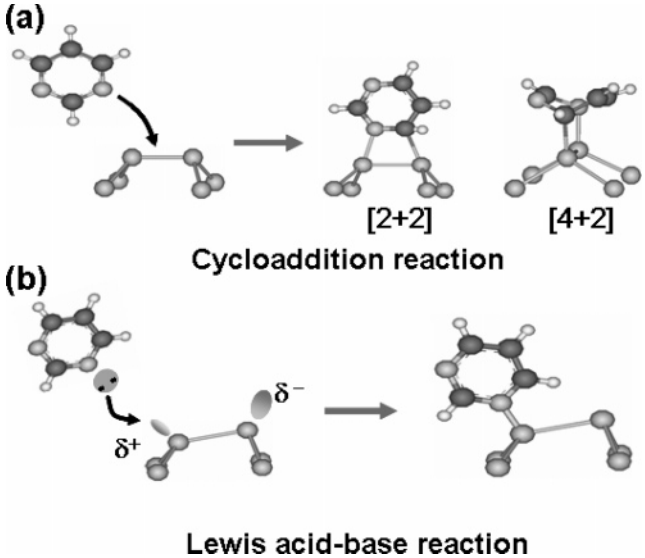

Figure 1. Models of the adsorption of pyrimidine onto a Ge(100) surface, in which pyrimidine binds to a Ge dimer via (a) a cycloaddition reaction or (b) a Lewis acid−base reaction. The black circles, gray circles, and small white circles in pyrimidine represent C, N, and H atoms, respectively, and the other gray circles represent Ge atoms.

* Corresponding authors. E-mail: sehun-kim@kaist.ac.kr (S.K.); hong@sejong.ac.kr (S.H.).
[†] Korea Advanced Institute of Science and Technology.
[‡] Sejong University.

10.1021/jp046947v CCC: $30.25
Published on Web 12/14/2004

A type of system of particular interest and potential importance consists of N-containing nucleic acid bases, such as pyrimidine or purine bases, adsorbed onto semiconductor (100) surfaces, which can be used as templates for attaching further organic molecules or biomolecules, such as amino acids, nucleic acids, or DNA, to semiconductor (100) surfaces.[19−21]

In this paper, we report STM, temperature-programmed desorption (TPD), and ab initio pseudopotential density-functional theory (DTF) studies of pyrimidine (1,3-diazine, $C_4H_4N_2$) molecules, one of the important parent molecules of nucleic acid bases, adsorbed onto a Ge(100) surface. Pyrimidine is a six-membered aromatic molecule with four carbon atoms and two nitrogen atoms, each with a lone pair of electrons.

Experimental and Theoretical Methods

Experimental Details. The experiments were performed in an ultrahigh vacuum (UHV) chamber at a base pressure below 2.0×10^{-10} Torr equipped with an OMICRON VT-STM instrument. A Ge(100) sample (p-type, $\rho = 0.10-0.39\ \Omega$) was cleaved to a size of 2×10 mm and mounted between two tantalum foil clips for STM measurements. The Ge(100) surface was cleaned using several cycles of sputtering with 1 keV Ar^+ ions for 20 min at 700 K, followed by annealing at 900 K for 10 min. The cleanliness of the Ge(100)-2×1 surface was checked with STM. An infrared optical pyrometer was used to measure the Ge(100) sample temperature. Pyrimidine ($C_4H_4N_2$, 99% purity) purchased from Aldrich was further purified by using several freeze−pump−thaw cycles to remove all dissolved gases prior to dosing. The purity of the pyrimidine was checked using mass spectrometry. Pyrimidine was introduced into the UHV chamber through a doser with a seven-capillary array controlled by a variable leak valve at room temperature. All STM images were recorded at a sample voltage between $V_s = -2.0$ and $+2.0$ V with a tunneling current of $I_t = 0.1$ nA using electrochemically etched W-tips. For the TPD experiments, a pyrimidine adsorbed Ge(100) surface was prepared, as described above for the STM experiments, in a UHV chamber equipped with a differentially pumped quadrupole mass spectrometer (QMS). The prepared sample was positioned about 2 mm away from the mass spectrometer aperture, which had a diameter of 3 mm. The heating rate used during the TPD measurements was 2 K/s.

Theoretical Calculations. Ab initio calculations were performed within the local density approximation (LDA) using the Vienna ab initio simulation package (VASP). The atoms were represented by ultrasoft pseudopotentials, as provided by VASP, and a kinetic energy cutoff of 224.5 eV was chosen. The Ge(100) surface with adsorbed pyrimidine was modeled as a slab composed of pyrimidine molecules, six Ge layers, and an H layer passivating the bottom surface. The positions of the atoms in the two bottom Ge layers and the H layer were fixed, while the other layers were relaxed with residual forces smaller than 0.01 eV/Å. Gaussian broadening with a width of 0.02 eV was used to accelerate the convergence in the *k*-point sum. Using self-consistent Kohn−Sham eigenvalues and wave functions, the constant-current STM images were simulated using the Tersoff−Hamann scheme.

Results and Discussion

A filled-state ($V_s = -1.8$ V) STM image of the clean Ge(100) surface is shown in Figure 2a. The image shows a defect-free surface consisting of symmetric dimer regions with 2×1 structure, and buckled dimer regions with c(4×2) structure. Figure 2b shows a filled-state ($V_s = -1.6$ V) STM image taken after adsorption of ~0.01 monolayer (ML) pyrimidine onto the clean Ge(100) surface at a substrate temperature of $T_s = 300$ K. The STM image contains several bright oval-shaped protrusions (one is indicated with an arrow), which can be attributed to adsorbed pyrimidine molecules. The oval-shaped protrusions, surrounded by six neighboring up-Ge atoms of buckled Ge dimers, are located between two Ge dimer rows. The STM image also shows that the symmetric dimer rows on the clean Ge(100)-2×1 surface are converted into buckled dimer rows after pyrimidine is adsorbed, indicating that adsorbed pyrimidine molecules induce buckling of the Ge dimer rows.

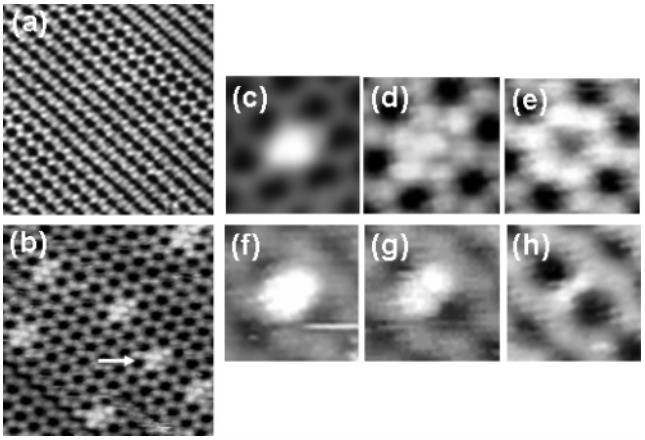

Figure 2. (a) A filled-state STM image (15×15 nm^2, $V_s = -1.8$ V, $I_t = 0.1$ nA) of a clean Ge(100) surface. (b) A filled-state STM image (15×15 nm^2, $V_s = -1.6$ V) of pyrimidine adsorbed onto a Ge(100) surface at a coverage of 0.01 ML. The arrow indicates an adsorbed pyrimidine molecule. STM images of pyrimidine on Ge(100) at various bias voltages, V_s: (c) −2.0 V, (d) −1.6 V, (e) −1.0 V, (f) +1.4 V, (g) +1.0 V, and (h) +0.8 V.

The STM image in Figure 2b confirms that the adsorbed pyrimidine molecules are attached to the down-Ge atoms of buckled Ge dimers by Ge−N dative bonding, as found in the pyridine/Ge(100) system. If pyrimidine molecules were covalently bonded to the Ge(100) surface as a result of [2+2] or [4+2] cycloaddition, the pyrimidine molecules would be located on top of the Ge dimers and the Ge dimers would be symmetric. However, such on-top configurations were not observed in the present work, although they have been observed in several previous studies.[6−10] The STM image indicates that pyrimidine molecules are attached either to the down-Ge atom of a Ge dimer by single dative bonding or to two down-Ge atoms of neighboring Ge dimer rows by double dative bonding. The bright oval-shaped protrusions are due to tunneling into the aromatic rings of the pyrimidine molecules. Hence, these STM results suggest that the adsorption of pyrimidine molecules onto Ge(100) surfaces proceeds via Lewis acid−base reactions between the lone pair of electrons of the N atoms in pyrimidine and the electron-deficient down-Ge atoms, which do not affect the aromaticity of the pyrimidine molecules. We obtained STM images of pyrimidine molecules adsorbed on Ge(100) for various bias voltages. Figure 2c−h shows STM images of the pyrimidine molecules recorded at the following bias voltages, V_s, (c) −2.0 V, (d) −1.6 V, (e) −1.0 V, (f) +1.4 V, (g) +1.0 V, and (h) +0.8 V, with the same tunneling current, $I_t = 0.1$ nA. The STM images of the adsorbed pyrimidine molecules can be seen to vary markedly with the bias voltage. In the empty-state images, the down-Ge atoms of the buckled dimers appear brighter than the up-Ge atoms, as reported previously,[22] in contrast to the filled-state images. The filled-state STM images in Figure 2c−e contain bright oval-shaped protrusions with a depressed Ge substrate at $V_s = -2.0$ V (Figure 2c), both oval-

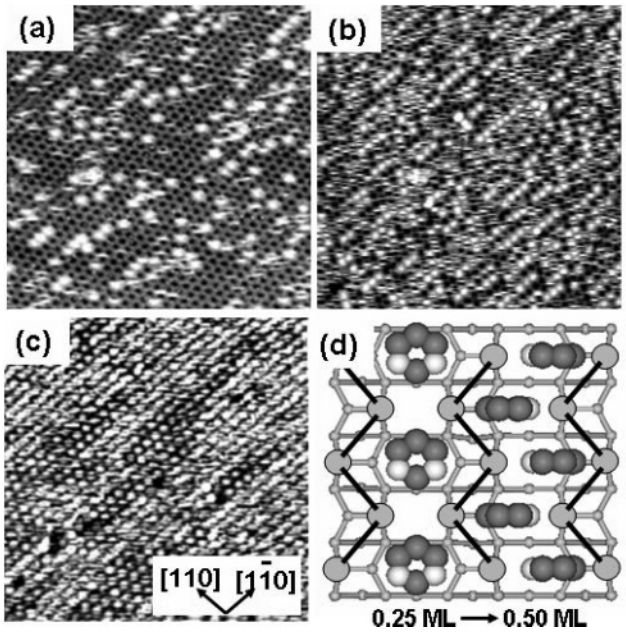

Figure 3. Filled-state STM images (30 × 30 nm^2, $V_s = -2.0$ V, $I_t = 0.1$ nA) of the Ge(100) surface after exposure to (a) 0.02 ML, (b) 0.10 ML, and (c) 0.35 ML of pyrimidine. Figure 3d depicts the phase transition from a c(4×2) structure to a p(2×2) structure due to the adsorption of pyrimidine.

shaped protrusions and the underlying substrate at $V_s = -1.6$ V (Figure 2d), and the underlying substrate without oval-shaped protrusions at $V_s = -1.0$ V (Figure 2e). However, the empty-state STM images recorded at $V_s = +1.0$ and $+0.8$ V show distinct molecular features, in particular, the double lobes in Figure 2g and h.

Figure 3a−c shows a series of STM images ($V_s = -2.0$ V) obtained for various pyrimidine coverages on the Ge(100) surface. In these STM images, we note that the Ge(100) surface is gradually saturated with oval-shaped protrusions and reconstructed into a c(4×2) structure at 0.25 ML coverage. However, with the dosing of pyrimidine above 0.25 ML shown in Figure 3c, the STM image contains a new feature, a bright zigzag line, which appears along the dimer row direction; for increasing coverages, the oval-shaped protrusions gradually change into brighter zigzag lines, and the Ge(100) surface is reconstructed into a p(2×2) structure. Figure 3d depicts the phase transition from the c(4×2) structure to the p(2×2) structure that occurs as a result of the adsorption of pyrimidine. At 0.25 ML coverage, we note that all pyrimidine molecules attach to the electron-deficient down-Ge atoms of every other Ge dimer along the [1$\bar{1}$0] direction through Lewis acid−base reactions. In the c(4×2) structure, the plane of adsorbed pyrimidine molecule is likely to be parallel to the surface due to interaction between π-bonds of pyrimidine and neighboring Ge dimers, as is found for the pyridine/Ge(100) system.[18] The interaction may allow the surface to be more stabilized resulting from additional stability due to the attractive interaction. The attachment of pyrimidine at down-Ge atoms in every Ge dimer forms the zigzag lines, resulting in the p(2×2) structure at 0.50 ML of pyrimidine coverage. The dimension of long axis in pyrimidine (4.91 Å) is larger than the distance (3.98 Å) between two neighboring Ge dimers along the dimer row. For the adsorption of pyrimidine at every Ge dimer, the plane of the adsorbed pyrimidine molecules changes from parallel to perpendicular to the surface to reduce the steric repulsion between them. However, the zigzag line (p(2×2)) structure is unstable due to repulsive interactions between neighboring pyrimidine molecules

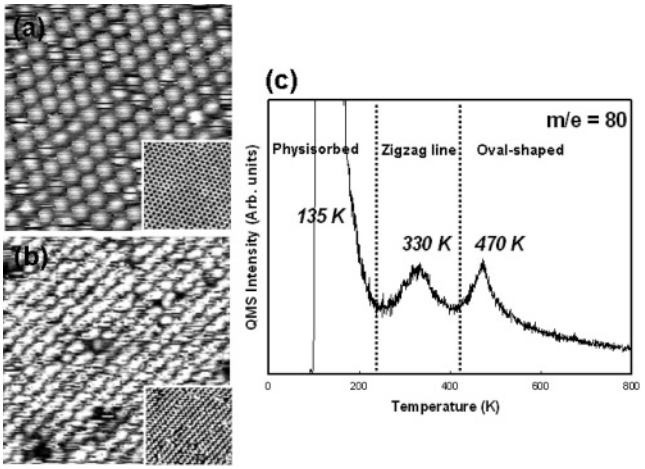

Figure 4. Filled-state STM images (15 × 15 nm^2, $V_s = -2.0$ V, $I_t = 0.1$ nA) of the Ge(100) surface at (a) 0.25 ML and (b) 0.50 ML of pyrimidine. The STM images in the insets were recorded at $V_s = -0.8$ V. A TPD spectrum of a pyrimidine-saturated Ge(100) surface at 100 K is shown in Figure 4c.

or between Ge atoms and the H atoms of the pyrimidine molecule. Thus, the structure is eventually transformed into oval-shaped protrusions (c(4×2)) spontaneously at room temperature within 30 min after stopping the exposure of pyrimidine to the surface.

Figure 4a and b shows filled-state ($V_s = -2.0$ V) STM images of the Ge(100) surface saturated with oval-shaped protrusions and zigzag lines, respectively, where the insets in Figure 4a and b are the corresponding filled-state images recorded at $V_s = -0.8$ V. The images show different regions of the surface. As explained above, we note that the Ge(100) surface shown in Figure 4a is reconstructed into the c(4×2) structure by the states that appear as oval-shaped protrusions, giving a well-ordered pyrimidine monolayer. The STM image in the inset of Figure 4a, which shows the underlying substrate without oval-shaped protrusions, was recorded at $V_s = -0.8$ V, and confirms that a regular c(4×2) structure forms over the entire region saturated with adsorbed pyrimidine molecules. Figure 4b shows that the Ge(100) surface is reconstructed into a p(2×2) structure by the adsorbed pyrimidine states that appear as fuzzy zigzag lines. The STM image in the inset of Figure 4b also shows a p(2×2) structure, except for some c(4×2) structure, over the entire region saturated with zigzag lines. A TPD spectrum for a pyrimidine-saturated Ge(100) surface at 100 K is shown in Figure 4c. During the thermal desorption experiments, mass peaks recorded were pyrimidine molecule ($C_4H_4N_2$) and its fragments. The spectrum consists of distinct desorption peaks at 330 and 470 K, as well as a peak at 135 K. In the region below ∼200 K, a peak at 135 K is discernible, which is attributed to the desorption of physisorbed pyrimidine. On the basis of the STM results, we attribute the two peaks at 330 and 470 K to the adsorbed pyrimidine states that appear as the weakly bound zigzag lines and the oval-shaped protrusions, respectively. We assume that those peaks result from the transition from the zigzag line state to the oval-shaped species state during the TPD measurements. These results imply that pyrimidine desorbs molecularly from the Ge(100) surface.

On the basis of the STM results discussed above, to investigate the adsorption configurations of pyrimidine on Ge(100), we carried out ab initio calculations within the local density approximation (LDA) using the Vienna ab initio simulation package (VASP).[23,24] The Ge(100) surface with adsorbed pyrimidine is modeled as a slab composed of pyrim-

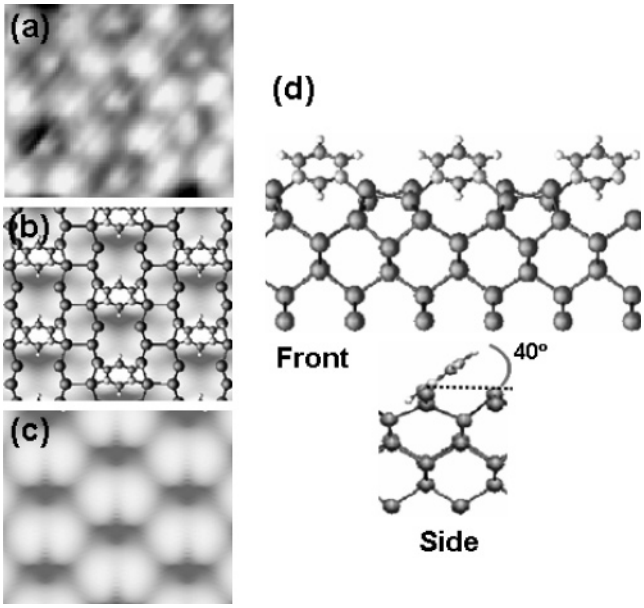

Figure 5. Comparison of (a) experimental (−1.6 V, 0.1 nA) and (b) theoretically calculated (−1.6 V) filled-state STM images of a Ge(100) surface at a pyrimidine coverage of 0.25 ML. The top view of the surface is overlapped with the simulated image. Distinct double lobes are seen in the calculated empty-state (+0.5 V) image in Figure 5c. Figure 5d shows the front and side views of the optimized structure.

idine molecules, six Ge layers, and a H layer passivating the bottom surface. The most stable adsorption structure arises when the pyrimidine molecule forms a bridge between two neighboring Ge dimer rows.

Figure 5a shows a filled-state ($V_s = -1.6$ V, $I_t = 0.1$ nA) STM image of the Ge(100) surface saturated with bright oval-shaped protrusions. Note that the Ge(100) surface is reconstructed into a c(4×2) structure at 0.25 ML by the states that appear as oval-shaped protrusions. Figure 5b and c shows theoretical calculations of (b) a filled-state image ($V_s = -1.6$ V) and (c) an empty-state image ($V_s = +0.5$ V) of the Ge(100) surface at a pyrimidine coverage of 0.25 ML. The simulated filled-state STM image in Figure 5b is in good agreement with the experimental STM image (Figure 5a). The empty-state image in Figure 5c shows a distinct double lobe, as seen in the STM image in Figure 2g. In this configuration, the pyrimidine molecule bridges between two down-Ge atoms in adjacent dimer rows. The calculations showed that (1) the Ge−N bond length (2.07 Å) is significantly longer than the length of the covalent bond between Ge and N atoms (1.70 Å), indicating that the pyrimidine molecules datively bind to the down-Ge atoms; (2) the plane of the pyrimidine molecules is tilted by about 40° with respect to the Ge surface and the molecules retain their aromaticity, as shown in Figure 5d; (3) the appearance of the double lobe in Figure 5c is mainly due to the character of the lowest unoccupied molecular orbital of the tilted pyrimidine molecule; and (4) an adsorption energy of 3.0 eV per pyrimidine is obtained for this tilted double dative bonding configuration, which is energetically favored by ∼0.6 eV over the tilted single dative bonding configuration and by ∼0.3 eV over the perpendicular double dative bonding configuration. In conjunction with the experimental observations, our results indicate that pyrimidine on Ge(100) has a tilted double dative bonding configuration.

Conclusion

The adsorption of pyrimidine onto the Ge(100)-2×1 surface has been investigated using STM, TPD, and DFT calculations. We conclude that the adsorbed pyrimidine molecules are tilted by about 40° with respect to the Ge surface and through a Lewis acid−base reaction form bridges between the down-Ge atoms of neighboring Ge dimer rows by double Ge−N dative bonding without loss of aromaticity. For coverages of pyrimidine up to 0.25 ML, a well-ordered c(4×2) structure results from the states that appear as oval-shaped protrusions, which correspond to pyrimidine molecules datively adsorbed on every other dimer. Above 0.25 ML, the oval-shaped protrusions are replaced by brighter zigzag lines. At 0.50 ML, a p(2×2) structure results from the states that appear as zigzag lines. The zigzag lines correspond to the adsorption of pyrimidine molecules on the down-Ge atoms of every Ge dimer. A TPD spectrum of pyrimidine-saturated Ge(100) at 100 K shows distinct desorption peaks at 330 and 470 K, as well as a peak at 135 K attributed to the desorption of physisorbed pyrimidine. We attribute the two peaks at 330 and 470 K to the adsorbed pyrimidine states that appear as the weakly bound zigzag lines and the oval-shaped protrusions, respectively. These weakly bound zigzag lines are eventually transformed into oval-shaped protrusions at room temperature because of steric hindrance between the adsorbed pyrimidine molecules.

Acknowledgment. This research was supported by grants from KOSEF through the Center for Nanotubes and Nanostructured Composites, the Brain Korea 21 Project, National R&D Project for Nano Science and Technology, and the Advanced Backbone IT Technology Development Project of the Ministry of Information and Communication. The calculations were supported by the KISTI through the 5th Strategic Supercomputing Support Program.

References and Notes

(1) Bent, S. F. *J. Phys. Chem. B* **2002**, *106*, 2830.
(2) Wolkow, R. A. *Annu. Rev. Phys. Chem.* **1999**, *50*, 413.
(3) Hamers, R. J.; Coulter, S. K.; Ellison, M. D.; Hovis, J. S.; Padowitz, D. F.; Schwartz, M. P.; Greenlief, C. M.; Russell, J. N., Jr. *Acc. Chem. Res.* **2000**, *33*, 617.
(4) Sun, Q.-Y.; de Smet, L. C. P. M.; van Lagen, B.; Wright, A.; Zuilhof, H.; Sudhölter, E. J. R. *Angew. Chem., Int. Ed.* **2004**, *43*, 1352.
(5) Wang, G. T.; Mui, C.; Musgrave, C. B.; Bent, S. F. *J. Phys. Chem. B* **2001**, *105*, 12559.
(6) Teague, L. C.; Boland, J. J. *J. Phys. Chem. B* **2003**, *107*, 3820.
(7) Teplyakov, A. V.; Kong, M. J.; Bent, S. F. *J. Am. Chem. Soc.* **1997**, *119*, 11100.
(8) Bitzer, T.; Rada, T.; Richardson, N. V. *J. Phys. Chem. B* **2001**, *105*, 4535.
(9) Filler, M. A.; Mui, C.; Musgrave, C. B.; Bent, S. F. *J. Am. Chem. Soc.* **2003**, *125*, 4928.
(10) Yoshinobu, J.; Tanaka, S.; Nishigima, M. *Jpn. J. Appl. Phys.* **1993**, *32*, 1171.
(11) Cao, X.; Coulter, S. K.; Ellison, M. D.; Liu, H.; Liu, J.; Hamers, R. J. *J. Phys. Chem. B* **2001**, *105*, 3759.
(12) Seino, K.; Schmidt, W. G.; Furthmüller, J.; Bechstedt, F. *Phys. Rev. B* **2002**, *66*, 235323-1.
(13) Tao, F.; Wang, Z. H.; Xu, G. Q. *J. Phys. Chem. B* **2002**, *106*, 3557.
(14) Cao, X.; Hamers, R. J. *J. Am. Chem. Soc.* **2001**, *123*, 10988l.
(15) Hossain, M. Z.; Machida, S.-I.; Yamashita, Y.; Mukai, K.; Yoshinobu, J. *J. Am. Chem. Soc.* **2003**, *125*, 9592.
(16) Tao, F.; Qiao, M. H.; Wang, Z. H.; Xu, G. Q. *J. Phys. Chem. B* **2003**, *107*, 6384.
(17) Mui, C.; Han, J. H.; Wang, G. T.; Musgrave, C. B.; Bent, S. F. *J. Am. Chem. Soc.* **2002**, *124*, 4027.
(18) Cho, Y. E.; Maeng, J. Y.; Kim, S.; Hong, S. *J. Am. Chem. Soc.* **2003**, *125*, 7514.
(19) Seino, K.; Schmidt, W. G.; Preuss, M.; Bechstedt, F. *J. Phys. Chem. B* **2003**, *107*, 5031.
(20) Chen, Q.; Richardson, N. V. *Nature* **2003**, *2*, 324.
(21) Kasaya, M.; Tabata, H.; Kawai, T. *Surf. Sci.* **1995**, *342*, 215.
(22) Qin, X. R.; Lagally, M. G. *Phys. Rev. B* **1999**, *59*, 7293.
(23) Kresse, G.; Hafner, J. *Phys. Rev. B* **1993**, *47*, 558.
(24) Kresse, G.; Furthmüller, J. *Phys. Rev. B* **1996**, *54*, 11169.